Reflectivity and transmissivity of an optical cavity coupled to two-level atoms: Coherence properties and the influence of atomic phase noise

B. Julsgaard* and K. Mølmer
Department of Physics and Astronomy, Aarhus University, Ny Munkegade 120, DK-8000 Aarhus C, Denmark.
(Dated: October 18, 2011)

We consider N identical two-level atoms coupled to an optical cavity, which is coherently driven by an external field. In the limit of small atomic excitation, the reflection and transmission coefficients for both fields and intensities are calculated analytically. In addition, the frequency content of the cavity field and hence also the emission spectrum of the cavity is determined. It is discussed in particular how individual collisional dephasing and common atomic energy-level fluctuations prevent the cavity field from being in a coherent state, which in turn affects the outgoing fields.

PACS numbers: 42.50.Ar, 42.50.Nn, 42.50.Pq

I. INTRODUCTION

In the field of cavity-quantum-electrodynamics, the coupling between a single two-level system and the electro-magnetic field is enhanced by a cavity, which allows for the study of light-matter interactions in the most fundamental way[1]. Such a setup has been implemented in various physical systems, e.g.: A Rydberg atom coupled to a micro-wave cavity[2], an alkali atom coupled to an optical cavity[3,4], a super-conducting qubit coupled to a transmission line resonator[5–7], and a semi-conductor quantum dot coupled to a photonic-crystal cavity[8,9]. Ensembles of two-level atoms, each coupled weakly to the cavity field, are also able to present an effective strong cooperative coupling[10–12]. The light-matter coupling gives rise to a normal-mode splitting of the resonance frequencies [known as the vacuum-Rabi splitting as explained by the Jaynes-Cummings model[13] for a single atom], which can be detected dynamically as oscillations between atomic and optical excitations[2], as a double-peak in the steady-state fluorescence spectrum[14], or as a doublet structure in the cavity-transmission profile[15]. The transmitted and reflected fields can be exploited in real-time detection and control of trapped atoms[16,17], and the reflection and transmission profile of these fields has previously been calculated using both classical[15] and quantum theories[18]. While the atomic-dipole-moment decay was most likely lifetime limited in the traditional experiments with free atoms in vacuum[2–4], the modern solid-state implementation has called for an increased attention to dephasing mechanisms in the case of both fluorescence[19] and transmission measurements[20]. The present work derives analytical expressions for the transmitted and reflected intensities, which under the influence of atomic dephasing noise do not coincide with the modulus square of the transmitted and reflected fields. In addition, the spectrum of the field emitted from the cavity is determined.

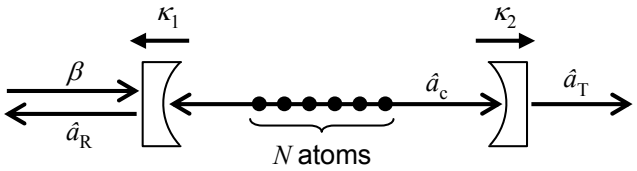

FIG. 1. The schematics of the physical system under consideration. An optical cavity contains a cavity field, $\hat{a}_c$, which couples equally to N two-level atoms. The field-decay rates through the two mirrors are denoted by κ_1 and κ_2, which connect the cavity field to the coherent input field, β, the reflected field, $\hat{a}_R$, and the transmitted field, $\hat{a}_T$.

II. AN EMPTY CAVITY WITH PHASE NOISE

Before considering the real problem of a cavity containing N atoms subjected to various decay processes, we wish to motivate the efforts by a simpler example: An empty cavity subjected to phase noise and driven coherently by the field $\beta_{in} = \beta e^{-i\omega_L t}$ (Fig. 1 without atoms, $N = 0$). In the frame rotating at the driving frequency, ω_L, the Hamiltonian of this simple system is given by:

$$\hat{H} = \hbar\Delta_c \hat{a}_c^\dagger \hat{a}_c + i\hbar\sqrt{2\kappa_1}(\beta \hat{a}_c^\dagger - \beta^* \hat{a}_c^\dagger), \qquad (1)$$

where $\Delta_c = \omega_c - \omega_L$ is the detuning from the cavity resonance frequency, ω_c. The input field amplitude, β, is normalized such that $|\beta|^2$ is the number of photons incident on the cavity input mirror per second, and the field-decay rate, κ_1, at the input mirror connects the cavity field, $\hat{a}_c$, to the incident and reflected fields, β and $\hat{a}_R$, by the input-output formalism of Collett and Gardiner[21]:

$$\begin{aligned} \hat{a}_R &= \sqrt{2\kappa_1}\hat{a}_c - (\beta + \hat{v}_1), \\ \hat{a}_T &= \sqrt{2\kappa_2}\hat{a}_c - \hat{v}_2. \end{aligned} \qquad (2)$$

The second line determines the transmitted field, $\hat{a}_T$, using the field-decay rate, κ_2, of the output mirror. In the above equations $\hat{v}_1$ and $\hat{v}_2$ operate on vacuum states and

will have no further impact on the calculations. In order to account for decay processes, we take the approach of the master equation, $\frac{\partial\rho}{\partial t} = \frac{1}{i\hbar}[\hat{H},\rho] + \mathcal{L}(\rho)$, where the Lindblad part, $\mathcal{L}(\rho)$, is a sum of terms:

$$\mathcal{L}_m(\rho) = -\frac{1}{2}(C_m^\dagger C_m\rho + \rho C_m^\dagger C_m) + C_m\rho C_m^\dagger. \quad (3)$$

The leakage of photons from the cavity is modeled by a Lindblad term with $C_1 = \sqrt{2\kappa}\hat{a}_\mathrm{c}$, where $\kappa = \kappa_1 + \kappa_2$ is the total cavity-field decay rate.

Now, we wish to include phase noise in the cavity. Physically, this could arise from a fast jitter of one of the mirrors such that the cavity resonance frequency becomes $\omega_\mathrm{c}' = \omega_\mathrm{c} + \varepsilon(t)$, where $\varepsilon(t)$ is a real function fulfilling $\langle\varepsilon(t)\rangle = 0$, and $\langle\varepsilon(t)\varepsilon(t')\rangle = \frac{2}{\tau_\mathrm{jit}}\delta(t-t')$. Computationally, the time-dependent term, $\hat{H}_\mathrm{jit} = \hbar\varepsilon(t)\hat{a}_c^\dagger\hat{a}_c$, could be added to the Hamiltonian; however, the fact that the noise is delta-correlated enables a simpler, time-independent modeling using a Lindblad term with $C_2 = \sqrt{\frac{2}{\tau_\mathrm{jit}}}\hat{a}_\mathrm{c}^\dagger\hat{a}_\mathrm{c}$, see App. A. The master equation now leads to the dynamical equations for the cavity field and photon number:

$$\frac{\partial\langle\hat{a}_\mathrm{c}\rangle}{\partial t} = -(\Gamma + i\Delta_\mathrm{c})\langle\hat{a}_\mathrm{c}\rangle + \sqrt{2\kappa_1}\beta, \quad (4)$$

$$\frac{\partial\langle\hat{a}_\mathrm{c}^\dagger\hat{a}_\mathrm{c}\rangle}{\partial t} = -2\kappa\langle\hat{a}_\mathrm{c}^\dagger\hat{a}_\mathrm{c}\rangle + \sqrt{2\kappa_1}\left(\beta\langle\hat{a}_\mathrm{c}^\dagger\rangle + \beta^*\langle\hat{a}_\mathrm{c}\rangle\right), \quad (5)$$

where $\Gamma = \frac{1}{\tau_\mathrm{jit}} + \kappa$. In steady state, the mean field amplitude and photon number can be written:

$$\langle\hat{a}_\mathrm{c}\rangle = \frac{\sqrt{2\kappa_1}\beta}{\Gamma + i\Delta_\mathrm{c}}, \quad (6)$$

$$\langle\hat{a}_\mathrm{c}^\dagger\hat{a}_\mathrm{c}\rangle = \left(1 + \frac{1}{\kappa\tau_\mathrm{jit}}\right)|\langle\hat{a}_\mathrm{c}\rangle|^2. \quad (7)$$

This result is important for calculating the reflected $\hat{a}_\mathrm{R}^\dagger\hat{a}_\mathrm{R}$ or transmitted $\hat{a}_\mathrm{T}^\dagger\hat{a}_\mathrm{T}$ intensity using Eqs. (2), and it is evident that the introduction of phase noise ($\tau_\mathrm{jit} < \infty$) prevents the cavity-field steady state from being coherent, which would otherwise lead to the simpler relation, $\langle\hat{a}_\mathrm{c}^\dagger\hat{a}_\mathrm{c}\rangle = |\langle\hat{a}_\mathrm{c}\rangle|^2$. The gradual change from a coherent state, when the contribution $(\kappa\tau_\mathrm{jit})^{-1}$ to Eq. (7) increases from zero, is shown by the Wigner function[22] in Fig. 2. In our real N-atom problem to be discussed in the next section, the atoms will effectively add phase noise to the cavity field, and, similar to the present example, the transmitted and reflected intensities cannot simply be calculated as the modulus square of the field amplitudes. We note that the impact of phase noise in a cavity on the density matrix itself has been studied experimentally by Wang *et al.*[7].

III. A CAVITY FILLED WITH ATOMS

Now, consider the entire setup of Fig. 1 with N identical two-level atoms placed in the coherently driven optical cavity. In addition to the empty-cavity Hamiltonian of Eq. (1), we add the contribution from atoms:

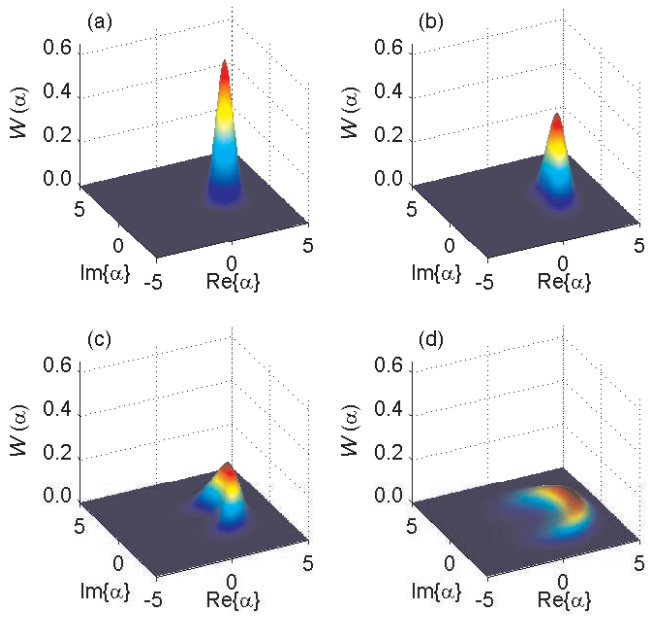

FIG. 2. The Wigner function for the cavity field for various contributions of phase noise. In all panels, $\langle\hat{a}_\mathrm{c}\rangle = 2$, and the value of $(\kappa\tau_\mathrm{jit})^{-1}$ is varied as: (a) 0.0, (b) 0.1, (c) 0.3, and (d) 1.0.

$$\hat{H}_\mathrm{atom} = \frac{\hbar\Delta_\mathrm{a}}{2}\sum_{j=1}^{N}\hat{\sigma}_z^{(j)} + \hbar g\sum_{j=1}^{N}(\hat{\sigma}_+^{(j)}\hat{a}_\mathrm{c} + \hat{\sigma}_-^{(j)}\hat{a}_\mathrm{c}^\dagger). \quad (8)$$

Here $\Delta_\mathrm{a} = \omega_\mathrm{a} - \omega_\mathrm{L}$ is the detuning of the driving frequency, ω_L, from the atomic resonance frequency, ω_a. The coupling constant, g, is taken to be equal for all atoms, the j'th of which is described by the Pauli operators, $\hat{\sigma}_k^{(j)}$ with $k = +,-,z$. We restrict the calculations to the regime of low excitation probability, $p_\mathrm{exc} = \frac{1}{2}(\langle\hat{\sigma}_z^{(j)}\rangle + 1) \ll 1$. This allows for the Holstein-Primakoff approximation, in which each atom is modeled by a harmonic oscillator:

$$\hat{\sigma}_-^{(j)} \to \hat{a}_j, \quad \hat{\sigma}_+^{(j)} \to \hat{a}_j^\dagger, \quad \hat{\sigma}_z^{(j)} \to 2\hat{a}_j^\dagger\hat{a}_j - 1. \quad (9)$$

With this approximation, the entire system Hamiltonian reads:

$$\begin{aligned}\hat{H} &= \hbar\Delta_\mathrm{c}\hat{a}_\mathrm{c}^\dagger\hat{a}_\mathrm{c} + \hbar\Delta_\mathrm{a}\sum_{j=1}^{N}\hat{a}_j^\dagger\hat{a}_j \\ &+ \hbar g\sum_{j=1}^{N}(\hat{a}_j^\dagger\hat{a}_\mathrm{c} + \hat{a}_j\hat{a}_\mathrm{c}^\dagger) + i\hbar\sqrt{2\kappa_1}(\beta\hat{a}_\mathrm{c}^\dagger - \beta^*\hat{a}_\mathrm{c}^\dagger),\end{aligned} \quad (10)$$

where the constant-energy shift from the -1-term in $\hat{\sigma}_z^{(j)}$ in (9) has been omitted. We assume that the phase noise from the jittering mirror (Sec. II) is absent ($\tau_\mathrm{jit} = \infty$,

i.e. $C_2 = 0$), but the cavity leakage is retained and various atomic decay processes will be included. Firstly, for each two-level atom the decay of population with rate $\gamma_\parallel$ is modeled by $C_3 = \sqrt{\gamma_\parallel}\hat{\sigma}_-^{(j)} \to \sqrt{\gamma_\parallel}\hat{a}_j$, where the arrow denotes the replacement suggested by Eq. (9). Secondly, dephasing of each individual atomic dipole moment is accounted for by $C_4 = \frac{1}{\sqrt{2\tau}}\hat{\sigma}_z^{(j)} \to \sqrt{\frac{2}{\tau}}\hat{a}_j^\dagger\hat{a}_j$, where τ is the dephasing rate[23] [the constant term -1 in (9) has been removed as it makes no contribution to the Lindblad operator (3) when C_m is hermitian]. Note that this Lindblad term can be derived as the average effect of fast random fluctuations of the resonance frequency of each atom along the lines of App. A. Due to the Holstein-Primakoff approximation, the above Lindblad terms, C_3 and C_4, for atomic-population decay and dipole-dephasing correspond exactly to the energy and phase decay in the harmonic oscillator[22]. Finally, in addition to individual atomic decay and dephasing processes, we add the possibility of dephasing mechanisms common to all atoms. For instance, a fluctuating magnetic field could vary the energy levels of an ensemble of magnetic dipoles in a uniform manner, and laser-intensity fluctuations could cause common energy-level variations of atoms in an optical dipole trap. This scenario is modeled by an additional fluctuating term in the Hamiltonian, $\hat{H}_1 = \hbar\varepsilon(t)\sum_j \hat{a}_j^\dagger\hat{a}_j$, where we assume the correlation time of fluctuations to be fast compared to any other time scale: $\langle\varepsilon(t)\rangle = 0$, and $\langle\varepsilon(t)\varepsilon(t')\rangle = \frac{2}{\tau'}\delta(t-t')$. As explained in App. A, such a fluctuating term can be cast into Lindblad form (3) with $C_5 = \sqrt{\frac{2}{\tau'}}\sum_j \hat{a}_j^\dagger\hat{a}_j$.

Based on the results in Sec. II, we expect atomic phase noise to destroy the coherence of the cavity field. Conversely, in absence of phase noise ($\tau = \tau' = \infty$) but maintaining population decay ($\gamma_\parallel > 0$), the cavity field is indeed coherent with $\langle\hat{a}_c^\dagger\hat{a}_c\rangle = |\langle\hat{a}_c\rangle|^2$ provided that the Holstein-Primakoff approximation holds. To see this, observe that the Hamiltonian (10) is on the form $\hat{H} = \sum_{j,k} q_{j,k}\hat{a}_j^\dagger\hat{a}_k$, where j,k are indices for atoms, the cavity, and the external (c-number) driving field, and $q_{j,k}$ are time-independent complex numbers. In the Heisenberg picture: $\frac{\partial}{\partial t}\hat{a}_j(t) = \frac{1}{i\hbar}\sum_k q_{j,k}\hat{a}_k(t)$, which in turn means that the vector $\hat{\vec{a}}$ of all annihilation operators, $\hat{a}_j$, evolve as $\hat{\vec{a}}(t) = \exp(-\frac{i}{\hbar}\mathbf{Q}t)\hat{\vec{a}}(0)$, where $\mathbf{Q}$ is the matrix of entries $q_{j,k}$. Now, if at time $t = 0$ all oscillators are in a coherent state with amplitudes $\vec{\alpha}$ (e.g. all atoms and the cavity in the vacuum state and the external driving field in a coherent state with amplitude β) such that $\hat{\vec{a}}(0)|\psi\rangle = \vec{\alpha}|\psi\rangle$, we find at later times: $\hat{\vec{a}}(t)|\psi\rangle = \exp(-\frac{i}{\hbar}\mathbf{Q}t)\hat{\vec{\alpha}}|\psi\rangle$, i.e. the state remains an eigenstate for all annihilation operators, and in particular the steady state of each oscillator must be coherent. Of course, this observation holds in the Schrödinger picture as well. Now, if population decay (with rate γ_j) of an oscillator is introduced, i.e. the Lindblad term with $C = \sqrt{\gamma_j}\hat{a}_j$ is included in the calculations, the evolution can be interpreted in the Schrödinger picture by the Monte-Carlo-wave-function approach[23]. This method states that the wave function should evolve under the non-Hermitian Hamiltonian, $\hat{H} - \frac{i\hbar}{2}\gamma_j\hat{a}_j^\dagger\hat{a}_j$, and occasionally be subjected to a quantum jump, $|\psi\rangle \to \hat{a}_j|\psi\rangle = \alpha_j|\psi\rangle$. The latter clearly preserves $|\psi\rangle$, and the non-Hermitian term is of the form discussed above and thus also preserves the coherent state.

IV. STEADY-STATE SOLUTIONS

A. Exact expressions

In order to calculate the relevant physical variables in steady state, the dynamical equations of the cavity field and atomic dipoles are deduced as a first step:

$$\frac{\partial\langle\hat{a}_c\rangle}{\partial t} = -(\kappa + i\Delta_c)\langle\hat{a}_c\rangle - ig\sum_{j=1}^{N}\langle\hat{a}_j\rangle + \sqrt{2\kappa_1}\beta, \quad (11)$$

$$\frac{\partial\langle\hat{a}_j\rangle}{\partial t} = -(\gamma_\perp + i\Delta_a)\langle\hat{a}_j\rangle - ig\langle\hat{a}_c\rangle, \quad (12)$$

where $\gamma_\perp = \frac{1}{\tau} + \frac{1}{\tau'} + \frac{\gamma_\parallel}{2}$. The steady state for the atomic operators becomes $\langle\hat{a}_j\rangle = \frac{-ig\langle\hat{a}_c\rangle}{\gamma_\perp + i\Delta_a}$, which in turn leads to the cavity-field steady-state value:

$$\langle\hat{a}_c\rangle = \frac{\sqrt{2\kappa_1}\beta}{(\kappa + i\Delta_c)(1+v)}, \quad v = \frac{g^2N}{(\kappa + i\Delta_c)(\gamma_\perp + i\Delta_a)}. \quad (13)$$

The complex field-reflection and transmission coefficients can be immediately deduced using Eq. (2):

$$r = \frac{\langle\hat{a}_R\rangle}{\beta} = \frac{2\kappa_1}{(\kappa + i\Delta_c)(1+v)} - 1 \quad (14)$$

$$t = \frac{\langle\hat{a}_T\rangle}{\beta} = \frac{2\sqrt{\kappa_1\kappa_2}}{(\kappa + i\Delta_c)(1+v)}. \quad (15)$$

These equations incorporate the dephasing mechanism through the definition of $\gamma_\perp$ and have been presented previously[15,18]. However, a correct treatment of intensities requires the computation of the number of photons in the cavity. To this end, we deduce the following equa-

tions of motions:

$$\frac{\partial}{\partial t}\left\langle \hat{a}_{\rm c}^{\dagger}\hat{a}_{\rm c}\right\rangle = -2\kappa\left\langle \hat{a}_{\rm c}^{\dagger}\hat{a}_{\rm c}\right\rangle + \sqrt{2\kappa_1}\left[\beta\left\langle \hat{a}_{\rm c}^{\dagger}\right\rangle + \beta^{*}\left\langle \hat{a}_{\rm c}\right\rangle\right] - ig\sum_{j=1}^{N}\left[\left\langle \hat{a}_{\rm c}^{\dagger}\hat{a}_{j}\right\rangle - \left\langle \hat{a}_{\rm c}\hat{a}_{j}^{\dagger}\right\rangle\right], \tag{16}$$

$$\frac{\partial}{\partial t}\left\langle \hat{a}_{\rm c}^{\dagger}\hat{a}_{j}\right\rangle = -\left(\kappa+\gamma_{\perp}+i\Delta_{\rm ac}\right)\left\langle \hat{a}_{\rm c}^{\dagger}\hat{a}_{j}\right\rangle + \sqrt{2\kappa_1}\beta^{*}\left\langle \hat{a}_{j}\right\rangle - ig\left\langle \hat{a}_{\rm c}^{\dagger}\hat{a}_{\rm c}\right\rangle + ig\sum_{k=1}^{N}\left\langle \hat{a}_{k}^{\dagger}\hat{a}_{j}\right\rangle, \tag{17}$$

$$\frac{\partial}{\partial t}\left\langle \hat{a}_{k}^{\dagger}\hat{a}_{j}\right\rangle = +ig\left[\left\langle \hat{a}_{\rm c}^{\dagger}\hat{a}_{j}\right\rangle - \left\langle \hat{a}_{\rm c}\hat{a}_{k}^{\dagger}\right\rangle\right] + 2\left\langle \hat{a}_{k}^{\dagger}\hat{a}_{j}\right\rangle\left[\frac{\delta_{k,j}-1}{\tau}-\frac{\gamma_{\parallel}}{2}\right], \tag{18}$$

where $\Delta_{\rm ac}=\Delta_{\rm a}-\Delta_{\rm c}$ has been defined. These equations can be solved in steady state [the details are presented in App. B]:

$$\left\langle \hat{a}_{\rm c}^{\dagger}\hat{a}_{\rm c}\right\rangle = \left[1+\frac{4g^4N(\kappa+\gamma_{\perp})}{(\gamma_{\perp}^2+\Delta_{\rm a}^2)\cdot D}\cdot\frac{\frac{\gamma_{\perp}}{\tau}+\frac{N\gamma_{\parallel}}{2\tau'}}{\frac{1}{\tau}+\frac{\gamma_{\parallel}}{2}}\right]|\left\langle \hat{a}_{\rm c}\right\rangle|^2, \tag{19}$$

$$p_{\rm exc} = \frac{2g^2|\left\langle \hat{a}_{\rm c}\right\rangle|^2\frac{\gamma_{\perp}}{\gamma_{\parallel}}}{\gamma_{\perp}^2+\Delta_{\rm a}^2}\left[1-\frac{4\kappa g^2(\kappa+\gamma_{\perp})}{\gamma_{\perp}\cdot D}\cdot\frac{\frac{\gamma_{\perp}}{\tau}+\frac{N\gamma_{\parallel}}{2\tau'}}{\frac{1}{\tau}+\frac{\gamma_{\parallel}}{2}}\right], \tag{20}$$

where D is a constant given by:

$$D = 2\kappa\gamma_{\parallel}[(\kappa+\gamma_{\perp})^2+\Delta_{\rm ac}^2] + 4\kappa g^2(\kappa+\gamma_{\perp})\left[\frac{1+\frac{N}{2}\gamma_{\parallel}\tau}{1+\frac{1}{2}\gamma_{\parallel}\tau}+\frac{N\gamma_{\parallel}}{2\kappa}\right]. \tag{21}$$

Equations (19) and (20) present one of the main results of the present paper; they determine the relevant properties of the coupled atom-cavity system, and with these at hand the intensity-reflection coefficient, $R=\left\langle \hat{a}_{\rm R}^{\dagger}\hat{a}_{\rm R}\right\rangle/|\beta|^2$, and the intensity-transmission coefficient, $T=\left\langle \hat{a}_{\rm T}^{\dagger}\hat{a}_{\rm T}\right\rangle/|\beta|^2$, can be stated using Eq. (2):

$$R = |r|^2+\frac{4\kappa_1^2}{\kappa^2+\Delta_{\rm c}^2}\frac{1}{|1+v|^2}\left(\frac{\left\langle \hat{a}_{\rm c}^{\dagger}\hat{a}_{\rm c}\right\rangle}{|\left\langle \hat{a}_{\rm c}\right\rangle|^2}-1\right), \tag{22}$$

$$T = |t|^2\cdot\frac{\left\langle \hat{a}_{\rm c}^{\dagger}\hat{a}_{\rm c}\right\rangle}{|\left\langle \hat{a}_{\rm c}\right\rangle|^2}. \tag{23}$$

Here r and t are the reflection and transmission coefficients, respectively, for the fields given by Eqs. (14) and (15), and the ratio $\left\langle \hat{a}_{\rm c}^{\dagger}\hat{a}_{\rm c}\right\rangle/|\left\langle \hat{a}_{\rm c}\right\rangle|^2$ is given by Eq. (19). In the absence of phase noise, this ratio is unity and the above expressions simplify into $R=|r|^2$ and $T=|t|^2$. In order to exemplify the practical impact of phase noise, consider Fig. 3, which shows the transmission profile for various decay parameters. In comparison to the case with no phase noise (dotted line), the transmission profile broadens and decreases in magnitude when phase noise is added (solid and dashed lines) since $\gamma_{\perp}$ increases from $\frac{\gamma_{\parallel}}{2}$ to $2\gamma_{\parallel}$, which in turn decreases the magnitude of $|t|^2$ in Eq. (23). However, the transmission remains higher than $|t|^2$ (open circles) due to the effect of Eq. (19), and this effect is larger for the common phase noise (dashed line) as compared to individual case (solid line). On a relative scale, this effect is most pronounced at $\omega_{\rm L}=0$ [at atomic resonance, $\Delta_{\rm a}=0$].

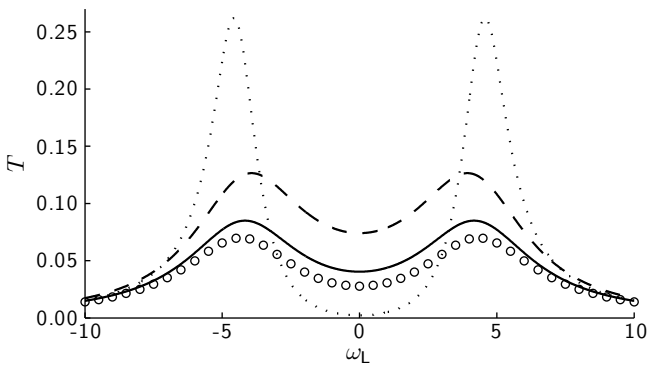

FIG. 3. The cavity intensity-transmission coefficient, T, as a function of driving frequency, $\omega_{\rm L}$. For all curves, $g=2$, $N=5$, $2\kappa_1=2\kappa_2=\kappa=1$, $\omega_{\rm a}=\omega_{\rm c}=0$, and $\gamma_{\parallel}=2$. Dotted line: No phase noise ($\gamma_{\perp}=\frac{\gamma_{\parallel}}{2}$), dashed line: Only common phase noise ($\gamma_{\perp}=2\gamma_{\parallel}$), solid line: Only individual phase noise ($\gamma_{\perp}=2\gamma_{\parallel}$). The open circles show the modulus square of the field-transmission coefficient, $|t|^2$, when $\gamma_{\perp}=2\gamma_{\parallel}$.

B. Approximate results, limits

Equations (19) and (20) are quite involved, but they reduce to simpler forms in interesting limiting cases. Consider the fraction (which is common in both equations):

$$\frac{\frac{\gamma_{\perp}}{\tau}+\frac{N\gamma_{\parallel}}{2\tau'}}{\frac{1}{\tau}+\frac{\gamma_{\parallel}}{2}} = \begin{cases} 0 & \text{when } \tau=\tau'=\infty, \\ \tau^{-1}+(\tau')^{-1} & \text{when } N=1, \\ \tau^{-1} & \text{when } \tau'=\infty, \\ N(\tau')^{-1} & \text{when } \tau=\infty. \end{cases} \tag{24}$$

This shows, that in absence of phase noise ($\tau=\tau'=\infty$), the square brackets in Eqs. (19) and (20) reduce to unity. This confirms the coherent state of the cavity field, $\left\langle \hat{a}_{\rm c}^{\dagger}\hat{a}_{\rm c}\right\rangle=|\left\langle \hat{a}_{\rm c}\right\rangle|^2$, and Eq. (20) reduces to the semiclassical expression for the atomic excitation probability in a classical field [with Rabi frequency, $\chi=2g\left\langle \hat{a}_{\rm c}\right\rangle$]. In the case of one atom, $N=1$, there is no difference between common and individual phase noise, and the two decay channels can be considered effectively as a single channel with characteristic rate, $\tau^{-1}+(\tau')^{-1}$. If only one or the other type of dephasing is present [individual collision-like dephasing only ($\tau'=\infty$, $\tau<\infty$) *or* common dephasing only ($\tau=\infty$, $\tau'<\infty$)], its effect is proportional with the rate of the process, and for common phase noise it is enhanced by a factor N. If we

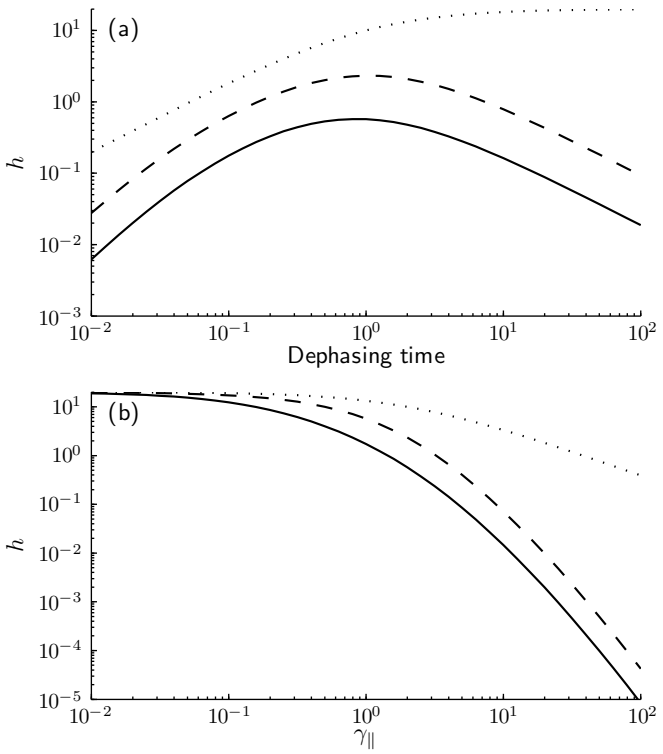

FIG. 4. Both panels show on the vertical scale the height, h, of the Lorentzian contribution: $\langle \hat{a}_c^\dagger \hat{a}_c \rangle = [1 + h \cdot \frac{\gamma_\perp^2}{\gamma_\perp^2 + \Delta_a^2}] \cdot |\langle \hat{a}_c \rangle|^2$, while the atomic decay parameters are varied. Solid line: Only individual phase noise ($\tau' = \infty$). Dashed line: Only common phase noise ($\tau = \infty$). The dotted line shows the cooperativity parameter $C = \frac{g^2 N}{\kappa \gamma_\perp}$. In panel (a) the dephasing time (τ or τ') is varied with $\gamma_\parallel = 2$. In panel (b) $\gamma_\parallel$ is varied with the dephasing time (τ or τ') set to unity. For both panels: $g = 2$, $N = 5$, $2\kappa_1 = 2\kappa_2 = \kappa = 1$, and $\Delta_{ac} = 0$.

write Eq. (19) as $\langle \hat{a}_c^\dagger \hat{a}_c \rangle = [1 + h \cdot \frac{\gamma_\perp^2}{\gamma_\perp^2 + \Delta_a^2}] \cdot |\langle \hat{a}_c \rangle|^2$, the pre-factor h of the Lorentzian function in Eq. (19) fulfills:

$$h \leq \begin{cases} C & \text{always,} \\ \frac{2C}{\gamma_\parallel} \left(\frac{1}{\tau'} + \frac{1}{N\tau} \right) & \text{when } \frac{1}{\tau}, \frac{1}{\tau'} \ll \frac{\gamma_\parallel}{2}, \end{cases} \tag{25}$$

where $C = \frac{g^2 N}{\kappa \gamma_\perp}$ is the cooperativity parameter. The maximum value C is obtained in the asymptotic limit $\gamma_\parallel \to 0$. The variations in h as a function of the atomic decay parameters is illuminated further in Fig. 4. In both panels, the cooperativity parameter C (dotted line) clearly presents an upper limit for h. Also, for these examples the common phase noise (dashed line) gives a larger contribution to h than individual phase noise (solid line) as indicated by Eq. (25), but otherwise present qualitatively similar features. In fact, when the decay is lifetime dominated ($\frac{\gamma_\parallel}{2} \gg \frac{1}{\tau}, \frac{1}{\tau'}$; right-hand-side limit of the two graphs) the height h decreases as (dephasing time)$^{-1}$ in panel (a) and as $\gamma_\parallel^{-2}$ in panel (b) as predicted by Eq. (25) [note, C scales as $\gamma_\parallel^{-1}$ in this limit]. Conversely, if the dephasing mechanisms dominate the lifetime decay ($\frac{\gamma_\parallel}{2} \ll \frac{1}{\tau}, \frac{1}{\tau'}$; left-hand-side limit of the two graphs), the cooperativity parameter C is the important figure of merit. In the limit $\gamma_\parallel \to 0$, one obtains $h \to C$ as exemplified in Fig. 4(b). This limit is reached whenever $\frac{\gamma_\parallel}{2} \ll \min \left\{ \kappa N^{-1},\ (N\tau)^{-1},\ \frac{g^2}{(\kappa + \gamma_\perp)(1 + \frac{\Delta_{ac}^2}{(\kappa + \gamma_\perp)^2})} \right\}$. For finite $\gamma_\parallel = 2$, as exemplified in Fig. 4(a), an approximate linear scaling of h with C is seen to apply.

V. THE CAVITY EMISSION SPECTRUM

The cavity field, $\hat{a}_c$, may possess frequency components different from the driving frequency, ω_L, when phase noise is present. The spectral density characterizes this effect:

$$S_{\hat{a}_c}(\omega) = \frac{1}{2\pi} \int_{-\infty}^{\infty} \langle \hat{a}_c^\dagger(t) \hat{a}_c(t+\tau) \rangle\, e^{i\Delta\tau} d\tau, \tag{26}$$

where $\Delta = \omega - \omega_L$ accounts for the rotating-frame picture of $\hat{a}_c$. Physically, $S_{\hat{a}_c}(\omega) d\omega$ measures how much optical energy is present in the cavity within a frequency bandwidth, $\delta\omega$, around ω. We note that $\int_{-\infty}^{\infty} S_{\hat{a}_c}(\omega) d\omega = \langle \hat{a}_c^\dagger \hat{a}_c \rangle$. With the computational details presented in App. C, the spectrum reads for an empty cavity subjected to phase noise (as described in Sec. II):

$$S_{\hat{a}_c}(\omega) = \left[\frac{\Gamma/\pi}{\Gamma^2 + (\omega_c - \omega)^2} \frac{1}{\kappa \tau_{jit}} + \delta(\omega - \omega_L) \right] |\langle \hat{a}_c \rangle|^2, \tag{27}$$

where $|\langle \hat{a}_c \rangle|^2$ refers to the steady-state cavity field depending on ω_L through Eq. (6). The spectrum is divided into two parts: A broad-band, incoherent Lorentzian term which is only present when the cavity is subjected to phase noise ($\tau_{jit} < \infty$), and a coherent part oscillating exactly at the driving frequency, ω_L. When atoms are included (as described in Sec. III) the spectrum becomes:

$$S_{\hat{a}_c}(\omega) = \left[\frac{(\kappa + \gamma_\perp)(\kappa\gamma_\perp + g^2 N) + \frac{\kappa \gamma_\perp \Delta_{ac}^2}{\kappa + \gamma_\perp}}{\pi |g^2 N + (\kappa + i[\omega_c - \omega])(\gamma_\perp + i[\omega_a - \omega])|^2} \times \frac{h \gamma_\perp^2}{\gamma_\perp^2 + (\omega_a - \omega_L)^2} + \delta(\omega - \omega_L) \right] |\langle \hat{a}_c \rangle|^2, \tag{28}$$

where h is the peak height discussed around Eq. (25). We remind that $h = 0$ in absence of phase noise. Once again, the spectrum is divided into a broad-band, in-

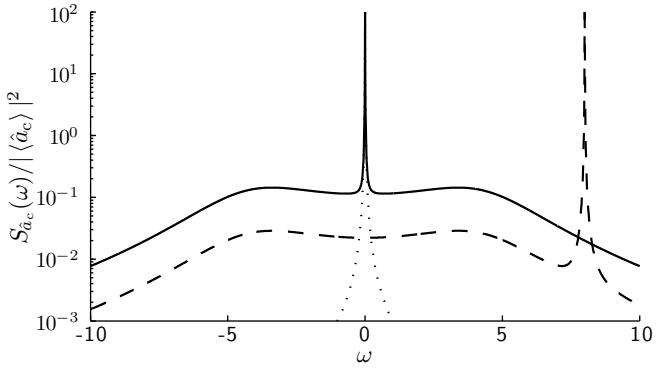

FIG. 5. The cavity emission spectrum [note the log scale] modeled with a resolution bandwidth of $\pi\kappa_{\rm p} = 10^{-2}$. For all curves, $g = 2$, $N = 5$, $2\kappa_1 = 2\kappa_2 = \kappa = 1$, $\omega_{\rm a} = \omega_{\rm c} = 0$, and $\gamma_\parallel = 2$. Solid and dashed lines: Only common phase noise ($\gamma_\perp = 2\gamma_\parallel$) with driving frequencies, $\omega_{\rm L} = 0$ and $\omega_{\rm L} = 8$, respectively. Dotted line: No phase noise, $\omega_{\rm L} = 0$.

coherent part and a delta-function term accounting for the coherent part. In both Eqs. (27) and (28), the left-most fraction in the square brackets is a function with unity area being proportional to $T(\omega) - |t(\omega)|^2$, where T and t are the intensity and field-transmission profiles, but with the driving frequency, $\omega_{\rm L}$, replaced by the observation frequency, ω. These fractions are then multiplied by the steady-state value of $\langle\hat{a}_{\rm c}^\dagger\hat{a}_{\rm c}\rangle - |\langle\hat{a}_{\rm c}\rangle|^2$ (the right-most fractions in the two equations together with $|\langle\hat{a}_{\rm c}\rangle|^2$), which thus becomes the area of the incoherent part of the spectrum. Due to the delta-functions, the coherent part contributes the remaining area, $|\langle\hat{a}_{\rm c}\rangle|^2$, such that the total area amounts to $\langle\hat{a}_{\rm c}^\dagger\hat{a}_{\rm c}\rangle$ as expected. Examples of spectra are presented in Fig. 5 with parameters closely resembling the dashed-line intensity-transmission profile of Fig. 3. As can be seen, it is only the magnitude of the incoherent spectrum which depends on the driving frequency, $\omega_{\rm L}$; its shape corresponds to the difference between the dashed line and the circles of Fig. 3. The sharp peaks resemble the coherent part, which follows $\omega_{\rm L}$. While the coherent part of the reflected and transmitted fields is related to the cavity field by the input-output relations Eq. (2), the incoherent, broad-band part of the spectrum is simply $2\kappa_1$ or $2\kappa_2$ times the incoherent cavity-field spectrum, $S_{\hat{a}_{\rm c}}(\omega)$, for the reflected and transmitted fields, respectively. We stress that the cavity emission spectrum [through its exit mirrors] depends on the field-correlation function, $\langle\hat{a}_{\rm c}^\dagger(t)\hat{a}_{\rm c}(t+\tau)\rangle$, and does not coincide with the atomic fluorescence spectrum[14], which is radiated into all space and depending on the atomic-dipole correlation function, $\langle\hat{\sigma}_+(t)\hat{\sigma}_-(t+\tau)\rangle$.

VI. DISCUSSION

The previous sections have identified the practical influence of atomic phase noise in two cases. Firstly, in a transmission or reflection measurement where the frequency, $\omega_{\rm L}$, of the coherent driving field is varied, the intensity-transmission and reflection profiles, $T(\omega_{\rm L})$ and $R(\omega_{\rm L})$, do not coincide with the modulus square of field-transmission and reflection profiles, $|t(\omega_{\rm L})|^2$ and $|r(\omega_{\rm L})|^2$, according to Eqs. (22) and (23). As a result, the pure dephasing-part of the atomic decay processes can be identified in experiment by e.g. comparing T and $|t|^2$, since the ratio should present a Lorentzian feature, $\frac{T}{|t|^2} = 1 + \frac{h\cdot\gamma_\perp^2}{\gamma_\perp^2+\Delta_{\rm a}^2}$, provided that the cooperativity parameter is not negligible. The transmitted intensity can be deduced simply by using a photo-detector, whereas the value of $|t|^2$ could be determined from measuring two orthogonal quadratures of the transmitted field in a homodyne detection setup. Secondly, for a fixed driving frequency, $\omega_{\rm L}$, the frequency content of the transmitted field can be determined by connecting the output of a photo-detector to a spectrum analyzer and searching for the broad-band, incoherent part as exemplified in Fig. 5.

We remind that all calculations of the present paper are only valid in the linear regime, i.e. when atomic excitation is small, which can be confirmed theoretically by using Eq. (20), or experimentally by observing that transmission or reflection properties are independent of the intensity of the driving field, β.

VII. CONCLUSION

For an optical cavity coupled to N two-level atoms, the steady-state reflection and transmission coefficients for both fields and intensities have been calculated analytically as a function of the frequency, $\omega_{\rm L}$, of a coherent driving field, assuming small atomic saturation. In addition, the frequency spectrum of the field emitted from the cavity has been determined. It has been demonstrated that atomic dephasing noise, independently subjected to each atom or common to all, prevents the cavity field from being in a coherent state, with two practical implications: (1) intensities do not coincide with the modulus square of the field amplitudes, and (2) a broad-band, incoherent part emerges in the cavity-emission spectrum.

ACKNOWLEDGMENTS

The authors acknowledge support from the EU integrated project AQUTE and the EU 7th Framework Programme collaborative project iQIT.

Appendix A: Transforming a rapidly fluctuating Hamiltonian to a Lindblad phase damping term

This appendix derives the Lindblad form of a phase decay, which is caused by a fast fluctuating term in the Hamiltonian. Consider the simple system: $\hat{H} = \hbar\varepsilon(t)\hat{O}$,

where $\varepsilon(t)$ is a real function fulfilling: $\langle\varepsilon(t)\rangle = 0$ and $\langle\varepsilon(t)\varepsilon(t')\rangle = D\delta(t-t')$, and $\hat{O}$ is a time-independent hermitian operator. The time evolution operator is given by: $\hat{U}(t_1,t_0) = \exp(-i\hat{O}\int_{t_0}^{t_1}\varepsilon(t)dt)$, which in turn evolves the density matrix as: $\rho(t_1) = \hat{U}(t_1,t_0)\rho(t_0)\hat{U}^\dagger(t_1,t_0)$. By expanding the time-evolution operator to second order (which makes sense when $t_1 - t_0$ is sufficiently small):

$$\hat{U}(t_1,t_0) \approx 1 - i\hat{O}\int_{t_0}^{t_1}\varepsilon(t)dt - \frac{1}{2}\hat{O}^2\int_{t_0}^{t_1}\int_{t_0}^{t_1}\varepsilon(t)\varepsilon(t')dtdt', \tag{A1}$$

it is possible to express the density matrix as:

$$\begin{aligned}\rho(t_1) &\approx \rho(t_0) - i[\hat{O},\rho(t_0)]\int_{t_0}^{t_1}\varepsilon(t)dt - \frac{1}{2}\int_{t_0}^{t_1}\int_{t_0}^{t_1}\varepsilon(t)\varepsilon(t')dtdt'\left[\hat{O}^2\rho(t_0) + \rho(t_0)\hat{O}^2 - 2\hat{O}\rho(t_0)\hat{O}\right] \\ &\to \rho(t_0) - \frac{D}{2}(t_1-t_0)\left[\hat{O}^2\rho(t_0) + \rho(t_0)\hat{O}^2 - 2\hat{O}\rho(t_0)\hat{O}\right],\end{aligned} \tag{A2}$$

where the arrow denotes averaging over the fast fluctuations of $\varepsilon(t)$. Now, by taking the limit, $t_1 \to t_0$, we reach the standard Lindblad form of Eq. (3) with $C = \sqrt{D}\hat{O}$.

Appendix B: Derivation of $\langle\hat{a}_c^\dagger\hat{a}_c\rangle$ and $p_{\rm exc}$

The steady-state solution of Eqs. (16)-(18) is derived in the following. Firstly, in Eq. (18) set $k = j$ and perform the summation over j. By adding the resulting right-hand side (which is zero in steady state) to Eq. (16), we obtain:

$$2\kappa\left\langle\hat{a}_c^\dagger\hat{a}_c\right\rangle + N\gamma_\parallel p_{\rm exc} = \sqrt{2\kappa_1}\left[\beta\left\langle\hat{a}_c^\dagger\right\rangle + \beta^*\left\langle\hat{a}_c\right\rangle\right], \tag{B1}$$

where $p_{\rm exc} = \frac{1}{N}\sum_j\left\langle\hat{a}_j^\dagger\hat{a}_j\right\rangle$ is the mean atomic excitation. The above equation states the conservation of energy: On the left-hand side the two terms describe the energy loss by cavity leakage and atomic population decay, which must be balanced by the right-hand side — the energy delivered by the coherent driving field. Secondly, an explicit expression for $\sum_{j,k}\left\langle\hat{a}_k^\dagger\hat{a}_j\right\rangle$ can be obtained from Eq. (18):

$$\sum_{j,k=1}^{N}\left\langle\hat{a}_k^\dagger\hat{a}_j\right\rangle = Np_{\rm exc}\frac{1+\frac{N}{2}\gamma_\parallel\tau}{1+\frac{1}{2}\gamma_\parallel\tau}. \tag{B2}$$

This can be inserted into Eq. (17) leading to an expression for $\sum_j\langle\hat{a}_c^\dagger\hat{a}_j\rangle$, which again is inserted into Eq. (18) [being summed over $j = k$]. As a result, another equation involving $\langle\hat{a}_c^\dagger\hat{a}_c\rangle$, $p_{\rm exc}$, and the already known cavity field $\langle\hat{a}_c\rangle$, is obtained, and we are left with two equations involving two unknowns:

$$\begin{bmatrix}a & b\\ c & d\end{bmatrix}\begin{bmatrix}p_{\rm exc}\\ \langle\hat{a}_c^\dagger\hat{a}_c\rangle\end{bmatrix} = \begin{bmatrix}e\\ f\end{bmatrix}|\langle\hat{a}_c\rangle|^2, \tag{B3}$$

where the constants a, b, c, d, e, and f are given by:

$$\begin{aligned}a &= \gamma_\parallel[(\kappa+\gamma_\perp)^2 + \Delta_{\rm ac}^2] + 2g^2(\kappa+\gamma_\perp)\frac{1+\frac{N}{2}\gamma_\parallel\tau}{1+\frac{1}{2}\gamma_\parallel\tau},\\ b &= -2g^2(\kappa+\gamma_\perp),\\ c &= N\gamma_\parallel,\\ d &= 2\kappa,\\ e &= \frac{2g^2}{\gamma_\perp^2+\Delta_{\rm a}^2}\{g^2N(\kappa+\gamma_\perp) + \kappa(\gamma_\perp^2 - \Delta_{\rm a}^2)\\ &\qquad + \gamma_\perp(\kappa^2+\Delta_{\rm c}^2) - 2\gamma_\perp\Delta_{\rm a}\Delta_{\rm c}\},\\ f &= 2\kappa + \frac{2\gamma_\perp g^2N}{\gamma_\perp^2+\Delta_{\rm a}^2}.\end{aligned} \tag{B4}$$

The determinant, $D = ad - bc$, of this set of equations was stated in Eq. (21). Now, $\langle\hat{a}_c^\dagger\hat{a}_c\rangle$ and $p_{\rm exc}$ can be deduced using Kramer's rule leading to the results of Eqs. (19) and (20).

Appendix C: Derivation of the cavity-field frequency spectrum

We present here the computational details for the cavity-field frequency spectrum, $S_{\hat{a}_c}(\omega)$. Since it is a measure of the frequency distribution of the optical energy, an actual measurement of this entity can be modeled by coupling (weakly) an auxiliary narrow-band probe cavity to the optical cavity and computing the steady-state photon number of the probe cavity. In other words, the physical system described by the Hamiltonian, $\hat{H}$, is extended to:

$$\hat{H}' = \hat{H} + \hbar\Delta\hat{a}_p^\dagger\hat{a}_p + \hbar g_p(\hat{a}_c^\dagger\hat{a}_p + \hat{a}_c\hat{a}_p^\dagger), \tag{C1}$$

where $\Delta = \omega - \omega_L$ denotes the observation frequency in the frame rotating at ω_L and g_p measures the strength of the coupling. In addition, the (half-width-half-maximum) bandwidth, κ_p, of the probe cavity is modeled by an extra Lindblad term with $C = \sqrt{2\kappa_p}\hat{a}_p$. In

steady state we derive:

$$\langle \hat{a}_{\rm p} \rangle = \frac{-i g_{\rm p} \langle \hat{a}_{\rm c} \rangle}{\kappa_{\rm p} + i\Delta}, \tag{C2}$$

which must be kept small for maintaining a negligible disturbance of the cavity field, $\hat{a}_{\rm c}$. By defining $g_{\rm p} \equiv \epsilon \kappa_{\rm p}$, the probe field is at least a factor of ϵ weaker than $\hat{a}_{\rm c}$ for any value of $\kappa_{\rm p}$ and Δ and it suffices to calculate $\langle \hat{a}_{\rm p}^\dagger \hat{a}_{\rm p} \rangle$ to second order in ϵ. Also, for a sufficiently small ϵ, the probe field $\hat{a}_{\rm p}$ can be truncated to the two lowest Fock states $\{|0\rangle_{\rm p}, |1\rangle_{\rm p}\}$ with $\hat{a}_{\rm p} = |0\rangle_{\rm p}\langle 1|_{\rm p}$, etc. The Hamiltonian $\hat{H}'$ and the entire density matrix ρ can then be expressed as:

$$\hat{H}' = \begin{bmatrix} \hat{H}^{00} & \hat{H}^{01} \\ \hat{H}^{10} & \hat{H}^{11} \end{bmatrix} = \begin{bmatrix} \hat{H} & \hbar g_{\rm p} \hat{a}_{\rm c}^\dagger \\ \hbar g_{\rm p} \hat{a}_{\rm c} & \hat{H} + \hbar\Delta \mathbf{1} \end{bmatrix}, \tag{C3}$$

and

$$\rho = \begin{bmatrix} \rho^{00} & \rho^{01} \\ \rho^{10} & \rho^{11} \end{bmatrix}. \tag{C4}$$

It follows that $\langle \hat{a}_{\rm p}^\dagger \hat{a}_{\rm p} \rangle = {\rm Tr}(\rho^{11})$ and $\langle \hat{a}_{\rm p} \rangle = {\rm Tr}(\rho^{10})$. Each of the four sub-blocks in $\hat{H}'$ have the dimensionality of the original, unperturbed system, $\hat{H}$, and the evolution can be written:

$$\begin{aligned} \frac{\partial \rho^{00}}{\partial t} =& \frac{1}{i\hbar}([\hat{H}^{00}, \rho^{00}] + \hat{H}^{01}\rho^{10} - \rho^{01}\hat{H}^{10}) \\ &+ \mathcal{L}(\rho^{00}) + 2\kappa_{\rm p}\rho^{11}, \end{aligned} \tag{C5}$$

$$\begin{aligned} \frac{\partial \rho^{10}}{\partial t} =& \frac{1}{i\hbar}(\hat{H}^{10}\rho^{00} + \hat{H}^{11}\rho^{10} - \rho^{10}\hat{H}^{00} - \rho^{11}\hat{H}^{10}) \\ &+ \mathcal{L}(\rho^{10}) - \kappa_{\rm p}\rho^{10}, \end{aligned} \tag{C6}$$

where $\mathcal{L}(\,\cdot\,)$ is the Lindblad super-operator of the original system and the probe-cavity decay is added separately. Now, in steady state set Eq. (C5) equal to zero and compute the trace:

$$\langle \hat{a}_{\rm p}^\dagger \hat{a}_{\rm p} \rangle = {\rm Tr}(\rho^{11}) = \frac{i\epsilon}{2}\left[{\rm Tr}(\hat{a}_{\rm c}^\dagger \rho^{10}) - {\rm Tr}(\hat{a}_{\rm c}\rho^{01})\right]. \tag{C7}$$

The value of ${\rm Tr}(\hat{a}_{\rm c}^\dagger \rho^{10})$ and its complex conjugate is required and may be deduced using Eq. (C6) [in steady state, multiply from the left by $\hat{a}_{\rm c}^\dagger$ and compute the trace]:

$$\begin{aligned} &\frac{1}{i\hbar}{\rm Tr}([\hat{a}_{\rm c}^\dagger, \hat{H}]\rho^{10}) + {\rm Tr}(\hat{a}_{\rm c}^\dagger \mathcal{L}(\rho^{10})) \\ &= (\kappa_{\rm p} + i\Delta){\rm Tr}(\hat{a}_{\rm c}^\dagger \rho^{10}) + i g_{\rm p} \langle \hat{a}_{\rm c}^\dagger \hat{a}_{\rm c} \rangle. \end{aligned} \tag{C8}$$

This equation has a great similarity with the steady-state equation for $\langle \hat{a}_{\rm c}^\dagger \rangle$. However, we must replace $\langle \hat{a}_{\rm c}^\dagger \rangle \to {\rm Tr}(\hat{a}_{\rm c}^\dagger \rho^{10})$, add an additional decay channel with rate $\kappa_{\rm p}$, introduce another detuning of Δ, and the extra term $i g_{\rm p} \langle \hat{a}_{\rm c}^\dagger \hat{a}_{\rm c} \rangle$ must be included. The progress from here depends on the actual physical system as defined by $\hat{H}$ and $\mathcal{L}$, but in practice the above-mentioned similarities allows for re-using existing equations in the spirit of the quantum regression theorem.

Now, in order to keep the derivations simple we adopt the physical system of Sec. II, i.e. an empty, coherently driven cavity subjected to phase noise. In similarity with Eq. (4), we obtain from Eq. (C8):

$$\begin{aligned} {\rm Tr}(\hat{a}_{\rm c}^\dagger \rho^{10}) &= \frac{-i g_{\rm p} \langle \hat{a}_{\rm c}^\dagger \hat{a}_{\rm c} \rangle + \sqrt{2\kappa_1}\beta^* {\rm Tr}(\rho^{10})}{\kappa_{\rm p} + \Gamma - i(\Delta_{\rm c} - \Delta)} \\ &= \frac{-i\epsilon\kappa_{\rm p}\left[\langle \hat{a}_{\rm c}^\dagger \hat{a}_{\rm c} \rangle + \frac{\Gamma - i\Delta_{\rm c}}{\kappa_{\rm p} + i\Delta} |\langle \hat{a}_{\rm c} \rangle|^2\right]}{\kappa_{\rm p} + \Gamma - i(\Delta_{\rm c} - \Delta)}, \end{aligned} \tag{C9}$$

where Eqs. (6) and (C2) were used in the second step — note we only require ${\rm Tr}(\hat{a}_{\rm c}^\dagger \rho^{10})$ to first order in ϵ, and hence the unperturbed values of $|\langle \hat{a}_{\rm c} \rangle|^2$ and $\langle \hat{a}_{\rm c}^\dagger \hat{a}_{\rm c} \rangle$ and also the relation (7) can be used. Now, insert the above result into Eq. (C7) and re-arrange the terms to obtain:

$$\frac{\langle \hat{a}_{\rm p}^\dagger \hat{a}_{\rm p} \rangle}{\pi \kappa_{\rm p} \epsilon^2} = \left[\frac{(\kappa_{\rm p} + \Gamma)/(\pi\kappa\tau_{\rm jit})}{(\kappa_{\rm p} + \Gamma)^2 + (\Delta_{\rm c} - \Delta)^2} + \frac{\kappa_{\rm p}/\pi}{\kappa_{\rm p}^2 + \Delta^2}\right] |\langle \hat{a}_{\rm c} \rangle|^2. \tag{C10}$$

The Lorentzian intensity-transmission profile of the probe cavity has an effective width [area-to-height ratio] of $\pi\kappa_{\rm p}$. Furthermore, since ϵ^2 connects the magnitudes of $|\langle \hat{a}_{\rm c} \rangle|^2$ and $|\langle \hat{a}_{\rm p} \rangle|^2$ through Eq. (C2), the left-hand side of the above expression can be interpreted as the amount of energy per frequency interval in the probe cavity when taking the limit $\kappa_{\rm p} \to 0$, which leads to Eq. (27). The case of atoms [Eq. (28)] can be derived in a similar fashion.

* Electronic mail: brianj@phys.au.dk

[1] H. J. Kimble, Physica Scripta **T76**, 127 (1998).

[2] M. Brune, F. Schmidt-Kaler, A. Maali, J. Dreyer, E. Hagley, J. M. Raimond, and S. Haroche, Phys. Rev. Lett. **76**, 1800 (1996).

[3] A. Boca, R. Miller, K. M. Birnbaum, A. D. Boozer, J. McKeever, and H. J. Kimble, Phys. Rev. Lett. **93**, 233603 (2004).

[4] P. Maunz, T. Puppe, I. Schuster, N. Syassen, P. W. H. Pinkse, and G. Rempe, Phys. Rev. Lett. **94**, 033002 (2005).

[5] A. Wallraff, D. I. Schuster, A. Blais, L. Frunzio, R. Huang, J. Majer, S. Kumar, S. M. Girvin, and R. J. Schoelkopf, Nature **431**, 162 (2004).

[6] F. Mallet, F. R. Ong, A. Palacios-Laloy, F. Nguyen, P. Bertet, D. Vion, and D. Esteve, Nature Phys. **5**, 791 (2009).

[7] H. Wang, M. Hofheinz, M. Ansmann, R. C. Bialczak, E. Lucero, M. Neeley, A. D. OConnell, D. Sank, M. Weides, J. Wenner, A. N. Cleland, and J. M. Martinis,

Phys. Rev. Lett. **103**, 200404 (2009).
[8] J. P. Reithmaier, G. Sek, A. Löffler, C. Hofmann, S. Kuhn, S. Reitzenstein, L. V. Keldysh, V. D. Kulakovskii, T. L. Reinecke, and A. Forchel, Nature **432**, 197 (2004).
[9] T. Yoshie, A. Scherer, J. Hendrickson, G. Khitrova, H. M. Gibbs, G. Rupper, C. Ell, O. B. Shchekin, and D. G. Deppe, Nature **432**, 200 (2004).
[10] P. F. Herskind, A. Dantan, J. P. Marler, M. Albert, and M. Drewsen, Nature Phys. **5**, 494 (2009).
[11] D. I. Schuster, A. P. Sears, E. Ginossar, L. DiCarlo, L. Frunzio, J. J. L. Morton, H. Wu, G. A. D. Briggs, B. B. Buckley, D. D. Awschalom, and R. J. Schoelkopf, Phys. Rev. Lett. **105**, 140501 (2010).
[12] Y. Kubo, F. R. Ong, P. Bertet, D. Vion, V. Jacques, D. Zheng, A. Dreau, J. F. Roch, A. Auffeves, F. Jelezko, J. Wrachtrup, M. F. Barthe, P. Bergonzo, and D. Esteve, Phys. Rev. Lett. **105**, 140502 (2010).
[13] E. T. Jaynes and F. W. Cummings, Proc. IEEE **51**, 89 (1963).
[14] J. J. Sanchez-Mondragon, N. B. Narozhny, and J. H. Eberly, Phys. Rev. Lett. **51**, 550 (1983).
[15] Y. Zhu, D. J. Gauthier, S. E. Morin, Q. Wu, H. J. Carmichael, and T. W. Mossberg, Phys. Rev. Lett. **64**, 2499 (1990).
[16] C. J. Hood, T. W. Lynn, A. C. Doherty, A. S. Parkins, and H. J. Kimble, Science **287**, 1447 (2000).
[17] P. W. H. Pinkse, T. Fischer, P. Maunz, and G. Rempe, Nature **404**, 365 (2000).
[18] M. Albert, J. P. Marler, P. F. Herskind, A. Dantan, and M. Drewsen, arXiv:1108.0528v1 (2011).
[19] A. Laucht, N. Hauke, J. M. Villas-Bôas, F. Hofbauer, G. Böhm, M. Kaniber, and J. J. Finley, Phys. Rev. Lett. **103**, 087405 (2009).
[20] K. Srinivasan and O. Painter, Nature **450**, 862 (2007).
[21] M. J. Collett and C. W. Gardiner, Phys. Rev. A **30**, 1386 (1984).
[22] C. W. Gardiner and P. Zoller, *Quantum Noise*, 2nd ed. (Springer, Berlin, 2000).
[23] K. Mølmer, Y. Castin, and J. Dalibard, J. Opt. Soc. Am. B **10**, 524 (1993).